



## The 65th ASH Annual Meeting Abstracts

## ONLINE PUBLICATION ONLY

## 622.LYMPHOMAS: TRANSLATIONAL-NON-GENETIC

**XPO1 Inhibitor Triggers Autophagy of TP53-Mutated Burkitt's Lymphoma Cells**Mowang Wang<sup>1,2</sup>, He Huang<sup>3,1</sup>, Limengmeng Wang<sup>2,1</sup>, Haowen Xiao<sup>4</sup><sup>1</sup>Liangzhu Laboratory, Zhejiang University Medical Center, HangZhou, China<sup>2</sup>Bone Marrow Transplantation Center, the First Affiliated Hospital, Zhejiang University School of Medicine, HangZhou, China<sup>3</sup>Bone Marrow Transplantation Center, The First Affiliated Hospital, Zhejiang University School of Medicine, Hangzhou, China<sup>4</sup>Department of Hematology, Sir Run Run Shaw Hospital, Zhejiang University, School of Medicine, Hangzhou, China**INTRODUCTION**

Burkitt lymphoma, a highly aggressive B-cell non-Hodgkin's lymphoma (NHL), has distinct pathological and clinical characteristics. Intensive combination chemotherapy has been widely used in the treatment of Burkitt lymphoma and survival has improved for Burkitt lymphoma patients. TP53 mutation frequency is not age related, and TP53 mutations are significantly associated with higher incidence of relapse. XPO1 inhibitors, novel targeted drugs, reversibly inhibit the nuclear export of tumor-associated proteins and mRNAs by blocking nuclear export protein 1 (XPO1). Preclinical and clinical studies of XPO1 inhibitors have been successfully used in treatment of AML, MM and NHL.

**METHODS**

We used CCK8 assays to detect growth inhibition in 4 lymphoma cell lines (Raji, Jeko-1, Daudi, and CA46) under the treatment of different concentrations of KPT330 (XPO1 inhibitor). The 4D-Label-free quantitative proteomics technology was used to determine the changes of protein distribution in the nucleoplasm and cytoplasm of CA46 cells before and after KPT330 treatment (50nM, 48h). The proteomic results were validated by QPCR, westernblotting assay and fluorescent marker analysis.

**RESULTS**

The lymphoma cell lines we choosed, Raji, Jeko-1, Daudi, and CA46, all have MYC rearrangement and TP53 mutations. CCK8 assay showed Jeko-1, Daudi and CA46 were relatively sensitive to KPT330 (IC50=86.87nM, 48.34nM and 87.85nM, respectively).

The results of the quantitative proteomics suggested proteins with increased nucleo-cytoplasmic ratio after KPT330 treatment were mainly focused on autophagy regulation and p53 signal pathways, including TFEB, USP10, DAP, NRBF2, SQSTM1, etc ( **Fig1, a**).

To confirm the effect of KPT330-triggered autophagy, first, we assessed the apoptosis rates of CA46 after exposure to KPT330 for 24 hours, all of which were below 10%, ruling out apoptosis-induced autophagy ( **Fig1, b**). Then, westernblotting results showed that the cytoplasm load of autophagy flux related proteins, LC3B-1 and LC3B-II, both increased after KPT330 treatment ( **Fig1, c**). To confirm whether KPT330 effects the generation or degradation of LC3B-II, we used the late autophagy inhibitor chloroquine (CQ) to cells and observed the p62 protein level reduced and LC3B-II protein level increased with additional use of CQ compared with only KPT330 treatment ( **Fig1, d**). Furthermore, the ratio of LC3B-II-CQ-presence to LC3B-II-CQ-absence in the KPT330-treated group was higher than that in the control group ( **Fig1, d**), suggesting that KPT330 may enhance the generation of LC3B-II. We further utilized the pLenti-CMV-mCherry-GFP-LC3B plasmid to establish an LC3B stable-overexpressing CA46 cell line. Flow cytometry analysis showed that the median fluorescence intensity of both GFP and mCherry signals increased after KPT330 treatment( **Fig1, e**), further confirming the overall elevation of LC3B levels.

To investigate the mechanism behind the increased autophagy flux, we utilized westernblotting analysis to validate the results from quantitative proteomics. TFEB protein level showed an increase in nuclear-cytoplasmic ratio upon KPT330 treatment ( **Fig2, a**). TFEB is known as a transcriptional activation protein, and its nuclear translocation is associated with the upregulated expression of genes involved in autophagosome formation, autolysosome fusion and lysosome biogenesis. QPCR analysis validated that genes associated with the aforementioned processes, such as LC3B, VPS11, CTSD, and CLCN7, exhibited increasing expression levels from 6 to 24 hours after KPT330 treatment ( **Fig2, b**). More interestingly, USP10, a component of

a regulatory loop that controls autophagy and p53/TP53 levels, significantly increased in cell nucleus after drug action ( **Fig2, c**), which suggested that KPT330 may stabilize p53 function.

Finally, we also attempted to discover the potential synergistic therapeutic effect of KPT330 with commonly used chemotherapy drugs in clinical lymphoma treatment. However, none synergistic effect was observed according to KPT330 combined with Cytarabine, Doxorubicin, Azacitidine, Decitabine, Rapamycin, Bortezomib, Duvelisib or Venetoclax, respectively ( **Fig2, d**).

### CONCLUSION

XPO1 Inhibitor, KPT330 can restrict nuclear export of autophagy-related proteins thus regulate autophagy and stabilize p53 function in TP53-mutated Burkitt's lymphoma cells, which revealed a promising treatment.

**Disclosures** No relevant conflicts of interest to declare.

Figure1

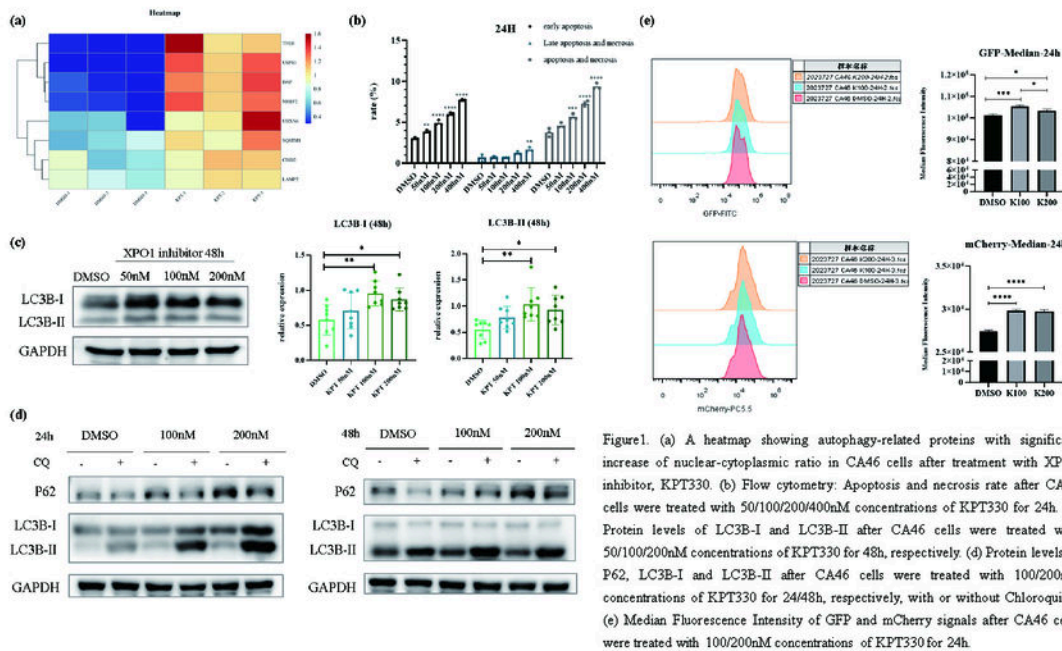


Figure1. (a) A heatmap showing autophagy-related proteins with significant increase of nuclear-cytoplasmic ratio in CA46 cells after treatment with XPO1 inhibitor, KPT330. (b) Flow cytometry. Apoptosis and necrosis rate after CA46 cells were treated with 50/100/200/400nM concentrations of KPT330 for 24h. (c) Protein levels of LC3B-I and LC3B-II after CA46 cells were treated with 50/100/200nM concentrations of KPT330 for 48h, respectively. (d) Protein levels of P62, LC3B-I and LC3B-II after CA46 cells were treated with 100/200nM concentrations of KPT330 for 24/48h, respectively, with or without Chloroquine. (e) Median Fluorescence Intensity of GFP and mCherry signals after CA46 cells were treated with 100/200nM concentrations of KPT330 for 24h.

Figure2

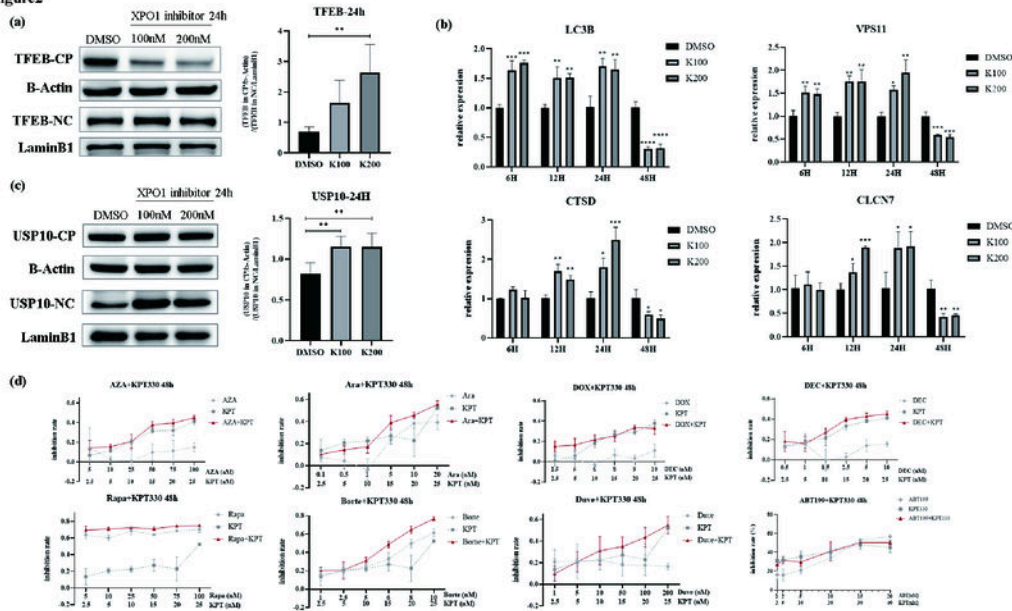


Figure2. (a) Left: Protein levels of TFEB after CA46 cells were treated with 100/200nM concentrations of KPT330 for 24h, respectively. Right: Nucleus-to-cytoplasm ratio columnar histogram of the TFEB protein. CP: cytoplasm; NC: nucleus. (b) Changes in the transcription levels of downstream genes related to autophagosomes, lysosomes and autophagolysosomes after CA46 cells were treated with 100/200nM KPT330 for 6-48 hours. (c) Left: Protein levels of USP10 after CA46 cells were treated with 100/200nM concentrations of KPT330 for 24h, respectively. Right: Nucleus-to-cytoplasm ratio columnar histogram of the USP10 protein. (d) CCK8 experiment investigating whether KPT330 has a synergistic inhibitory effect with Cytarabine, Doxorubicin, Azacitidine, Decitabine, Rapamycin, Bortezomib, Duvelisib and Venetoclax on CA46 cell line. The gray dashed line represents the inhibitory effect of the single drug, and the solid red line represents the inhibitory effect when the two drugs are used in combination. Ara: cytarabine; DOX: doxorubicin, AZA: azacitidine, DEC: decitabine, Rapa: Rapamycin, Borte: bortezomib, Duve: duvelisib, ABT199: venetoclax.

Figure 1

<https://doi.org/10.1182/blood-2023-188432>